Nonmonotonic inelastic tunneling spectra due to emission of surface magnons in itinerant electron ferromagnetic junctions

G. Tkachov
Institute for Theoretical Physics, Regensburg University, 93040 Regensburg, Germany
(Dated: February 2, 2008)

We propose an itinerant electron theory of nonmonotonic inelastic tunneling spectra of ferromagnetic junctions observed in several recent experiments. Assuming that the Coulomb interaction between electrons across the barrier is poorly screened due to the exponential suppression of the band electron density inside the barrier, we consider a process where a hot electron from one ferromagnet during the tunneling excites a magnon at the surface of the other ferromagnet in the course of the exchange scattering with a Fermi sea electron from the opposite side. For this process one can derive an inelastic transfer Hamiltonian in which the matrix elements of the electron-magnon coupling depend on the magnon wave-vector (and hence on its energy) via the long-range Coulomb potential. This dependence can account for the sharp peaks observed in the low-temperature tunneling spectra of a number of ferromagnetic junctions at the excitation energies much smaller than the Curie temperature of the ferromagnets.

PACS numbers: 72.25.Ba, 72.25.Rb, 73.40.Gk, 75.30.Ds, 75.30.Et

I. INTRODUCTION

Spin polarized transport in tunnel ferromagnetic junctions has been a subject of intense research[1] motivated by the desire to develop a form of electronics which utilizes the dependence of the junction resistance on the spin-polarization of carriers in the ferromagnets. Since ferromagnetic metals have more band electrons of one spin polarization (known as majority carriers) present at the Fermi energy E_F than of the inverse polarization (minority carriers), the resistance depends on the relative orientation of the magnetic moments in the ferromagnets which is controlled by an external weak magnetic field. With parallel magnetizations, the tunneling occurs between majority (and minority) bands whereas in a junction with antiparallel magnetizations carriers tunnel from majority to minority bands (and vice versa). The resulting spin current mismatch produces a larger contact resistance in the antiparallel case, an effect known as junction magnetoresistance (JMR)[2,3].

This simple picture was successful in interpreting current-voltage (I-V) characteristics at low bias voltage of the order of a *few* millivolts. For V about a *hundred* millivolts the JMR was found to be strongly reduced[4,5,6,7,8]. Since this energy scale is of the order of that of spin excitations (about the Curie temperature T_C of the ferromagnets), it was suggested that electrons tunneling from one ferromagnet with energies $\approx |eV|$ above the Fermi energy in the other ferromagnet (hot electrons) excite both surface[6] and bulk[9] magnons, so that the reduction in the resistance for the antiparallel alignment turns out to be bigger than for the parallel case leading to a decrease in the JMR. Within the framework of the transfer Hamiltonian model[10,11] and neglecting the energy dependence of the electron-magnon coupling, one can identify the nonlinear magnon-assisted contribution to the tunneling current by taking the second derivative d^2I/dV^2 which can be related at zero temperature to the magnon density of states Ω at the excitation energy $|eV|$[6,9]:

$$d^2I/dV^2 \propto \mathrm{sign}(V)\Omega(|eV|), \tag{1}$$

where e is the electron charge.

In the case of the bulk magnons, $\Omega \propto |eV|^{1/2}$, the inelastic contribution (1) vanishes for $V \to 0$ whereas for the surface ones the density of states is energy-independent, $\Omega = const$, and the second derivative (1) is discontinuous at $V = 0$. This corresponds to a cusp-like zero-bias anomaly in the conductance observed at low temperatures in a number of experiments[4,5,6,7,8] pointing to the dominant role of the surface magnons in the inelastic tunneling spectroscopy at excitation energies smaller than the Curie temperature.

In contrast with simple formula (1) real inelastic tunneling spectra are strongly nonmonotonic[8]. According to the data obtained in Ref. 8 for $Co/Al_2O_3/Ni_{80}Fe_{20}$ junctions, $d^2I(V)/dV^2$ has two antisymmetric sharp peaks at excitation energies much smaller than the Curie temperature of the ferromagnets. Similar results have been recently obtained in Refs. 12,13,14 for several types of junctions, showing that the nonmonotonic behaviour of the tunneling spectra is a generic feature of inelastic tunneling between ferromagnets. *In this paper* we propose a microscopic theory of magnon-assisted tunneling which links the nonmonotonic tunneling spectra to the energy dependence of the electron-magnon interaction. The magnon emission (absorption) processes are treated in the model of band electrons in the similar spirit as in Refs. 15,16

To anticipate, as the excitation energies of interest are quite small, we focus on the exchange processes accompanied by emission of surface magnons. They are snown schematically in Fig. 1 for the simplest case of fully-polarized ferromagnets with antiparallel magnetizations where elastic tunneling is forbidden. We assume that, due to the exponential suppression of the electron den-

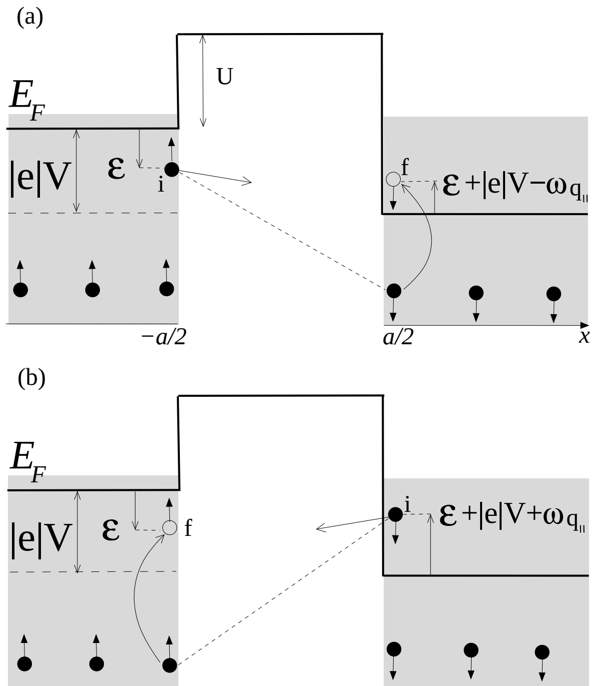

FIG. 1: Exchange-induced spin-flip tunneling between half-metallic ferromagnets with antiparallel magnetizations: (a) – while tunneling, a hot spin-up electron from the left-hand ferromagnet excites a Fermi sea spin-down electron from the opposite side into a state above the Fermi level. Although the tunneling electron cannot occupy any one-particle state in the right-hand ferromagnet, its presence on the right-hand side can be treated as an excitation of the collective spin of the Fermi sea (spin-down) electrons. (b) – temperature-stimulated counter exchange process due to the finite occupation number of the initial state with energy $\epsilon + |e|V + \omega_{\mathbf{q}_\parallel}$ above the Fermi level in the right-hand system. $\mathbf{q}_\parallel$ and $\omega_{\mathbf{q}_\parallel} \leq |e|V$ are the wave-vector and energy of a surface spin-wave; a and U are the barrier thickness and height, respectively.

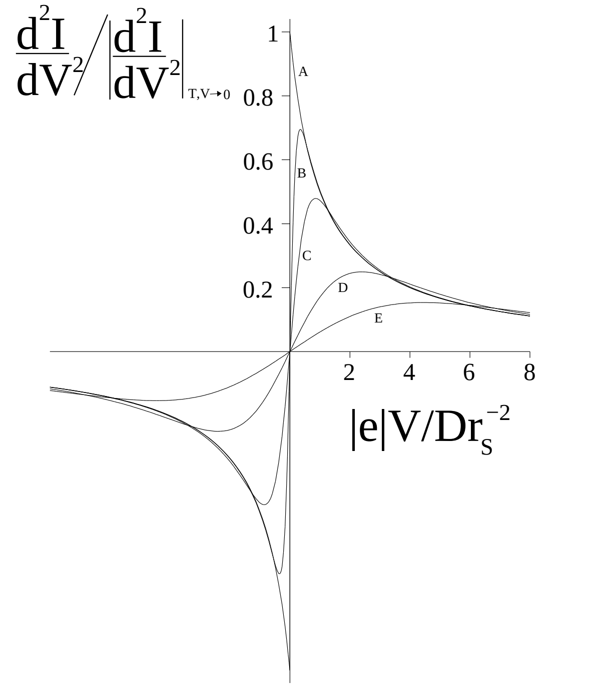

FIG. 2: Inelastic electron tunneling spectrum at different temperatures: (A) $k_BT/Dr_S^{-2} = 0$, (B) $k_BT/Dr_S^{-2} = 0.1$, (C) $k_BT/Dr_S^{-2} = 0.3$, (D) $k_BT/Dr_S^{-2} = 1$, (E) $k_BT/Dr_S^{-2} = 2$, where Dr_S^{-2} is the energy of a surface magnon with the wavelength equal to the screening radius.

sity inside the barrier, band electrons interact directly across the barrier via a long-range Coulomb potential which depends only on the distance between electrons in the interfacial plane with the screening radius r_S greater than the barrier thickness a. In the process shown in Fig. 1a the magnon emission occurs in the course of the exchange scattering between a hot spin-up electron from the left-hand ferromagnet and a Fermi sea spin-down electron from the right-hand system. The latter is excited into a state above the Fermi energy, leaving a hole inside the Fermi sea, whereas the former cannot occupy any one-particle state in the right-hand system because they are all spin-down ones. Collectively, however, the state of the "spin-down" Fermi sea with an electron having the wrong spin can be described as a spin-wave excitation[17] with wave-vector $\mathbf{q}_\parallel$ parallel to the boundary and energy $\omega_{\mathbf{q}_\parallel} \leq |e|V$. The contribution of such processes into the inelastic tunneling spectrum is characterized by the matrix elements of the electron-magnon coupling which depends on the magnon wave-vector via the Fourier transform of the Coulomb potential $\mathcal{V}(\mathbf{q}_\parallel) = 2\pi e^2/(r_S^{-2} + q_\parallel^2)^{1/2}$:

$$\frac{d^2I}{dV^2} = \left|\frac{d^2I}{dV^2}\right|_{T,V\to 0} \Omega^{-1} \sum_{\mathbf{q}_\parallel} \frac{\mathcal{V}^2(\mathbf{q}_\parallel)}{\mathcal{V}^2(0)} \int d\epsilon \times \tag{2}$$

$$\times \left[n'(\epsilon)n'(\epsilon + |e|V - \omega_{\mathbf{q}_\parallel}) - n'(\epsilon + |e|V + \omega_{\mathbf{q}_\parallel})n'(\epsilon)\right].$$

In the first term the Fermi occupation numbers $n(\epsilon)$ and $n(\epsilon + |e|V - \omega_{\mathbf{q}_\parallel})$ correspond to the initial (i) and final (f) electron states in the process shown in Fig. 1a. The second term comes from a similar exchange process (Fig. 1b) where in the initial state a spin-down electron has energy $\epsilon + |e|V + \omega_{\mathbf{q}_\parallel}$ above the Fermi level in the right-hand system whereas in the final state a spin-up electron has energy ϵ with respect to the Fermi level in the left-hand system. For positive bias voltage $V > 0$ this process is only possible at finite temperature T when the occupation number of the initial state $n(\epsilon + |e|V + \omega_{\mathbf{q}_\parallel})$ is not zero. In Eq. (2) $\Omega = A/4\pi D$ is the density of states of the surface magnons (proportional to the contact area A) and $\omega_{\mathbf{q}_\parallel} = Dq_\parallel^2$ is their dispersion relation with D being the spin stiffness. With magnon wave-vector dependence of the electron-magnon interaction, the second derivative of the tunneling current (2) has two antisymmetric peaks as a function of bias voltage (Fig. 2). As the

temperature increases, they broaden and shift to higher energies in a similar way as in the experiments[3,8,12,13,14]. The peak intensity in the limit of zero bias and temperature, $|d^2I/dV^2|_{T,V\to 0}$ can be expressed in terms of the barrier transparency and electron band parameters of the ferromagnets.

The paper is organized as follows. In sections II and III we propose a new simple method of deriving both tunneling current operator and transfer Hamiltonian for interacting electrons. Unlike the previous approaches to this problem[18,19,20], we derive effective microscopic boundary conditions for the "right" and "left" electrons at the barrier walls and show that they can be rewritten in the form of the transfer Hamiltonian in the coordinate representation. In section IV the results for the tunneling current between ferromagnets of arbitrary spin-polarization are discussed for both antiparallel and parallel alignment of their magnetic moments.

II. EFFECTIVE BOUNDARY CONDITIONS FOR THE "LEFT" AND "RIGHT" ELECTRONS

In this section we find an approximate solution of the equation of motion for the field operators of the interacting electrons inside the barrier and eliminate this region by deriving effective boundary conditions for the left and right operators at the barrier boundaries.

Consider a contact of a large area A between two ferromagnetic metals separated by a tunnel barrier characterized by the thickness a and the length of the electron penetration $\lambda = \hbar/(2mU)^{1/2}$ which depends on the barrier height U measured with respect to the chemical potential and the electron effective mass m (Fig. 1). For U of the order of the Fermi energy E_F in the metals[3,8], one can neglect the energy and momentum dependence of the electron penetration length. The thickness of the barrier a is normally much greater than λ and the density of band electrons inside the barrier, $\sim \mathrm{e}^{-a/\lambda} n_0$ is exponentially reduced compared to that in the leads n_0, leading to direct electron-electron interactions across the barrier via a long-range Coulomb potential. Unlike the case of Refs. 15,16, here we deal with tunneling accompanied by the interaction *inside the barrier*.

In order to treat such inelastic processes, we will use the Coulomb potential $\mathcal{V}(\mathbf{R}) = e^2 \mathrm{e}^{-R/r_s}/R$ with the screening radius $r_s \sim 1/(\mathrm{e}^{-a/\lambda} n_0)^{1/3}$ much greater than that in the metals ($\sim n_0^{-1/3}$), where $\mathbf{R} = \{x;\mathbf{r}\}$ with the x-axis perpendicular to the interface and the position vector in the interfacial plane $\mathbf{r}$. In the case of the experiments described in Refs. 3,8, r_s can be estimated as being greater than the thickness of the barrier a, which allows one to neglect the x-dependence of the Coulomb potential: $\mathcal{V}(\mathbf{r}) = e^2 \mathrm{e}^{-r/r_s}/r$. Out all of the inelastic processes we will only take into account those due to the exchange scattering of two electrons in the states with opposite spins α and $-\alpha$ since they are known to result in the exchange-induced spin excitations[17]. The exchange Hamiltonian

$$H_{ex} = -\sum_{\alpha,\mathbf{k}_2\neq\mathbf{k}_1+\mathbf{q}} \frac{\mathcal{V}_{\mathbf{k}_2-\mathbf{k}_1-\mathbf{q}}}{2A} \int_{-\frac{a}{2}}^{\frac{a}{2}} dx_1 dx_2 \times \tag{3}$$
$$\times \chi^{\dagger}_{\alpha\mathbf{k}_2-\mathbf{q}}(x_1)\chi_{-\alpha\mathbf{k}_2}(x_2)\chi^{\dagger}_{-\alpha\mathbf{k}_1+\mathbf{q}}(x_2)\chi_{\alpha\mathbf{k}_1}(x_1),$$

is written in terms of the operators $\chi_{\alpha\mathbf{k}}(x)$ and $\chi^{\dagger}_{\alpha\mathbf{k}}(x)$ annihilating and creating, respectively, an electron with spin α and wave-vector $\mathbf{k}$ parallel to the interface at point x inside the barrier (the index $\|$ is dropped from now on). The Fourier transform of the Coulomb potential is given by

$$\mathcal{V}_{\mathbf{q}} = 2\pi e^2 \int_0^{\infty} r dr \frac{\mathrm{e}^{-r/r_s}}{r} J_0(rq) = \frac{2\pi e^2}{(r_S^{-2}+q^2)^{1/2}}, \tag{4}$$

where $J_0(x)$ is the Bessel function. The equation of motion for $\chi_{\alpha\mathbf{k}}(x)$ can be written as

$$[\partial_x^2 - \lambda^{-2}]\chi_{\alpha\mathbf{k}}(x) = -\frac{2m}{\hbar^2 A}\sum_{\mathbf{k}_1\mathbf{q}} \mathcal{V}_{\mathbf{k}-\mathbf{k}_1} \times \tag{5}$$
$$\times \int_{-\frac{a}{2}}^{\frac{a}{2}} dx_1 \chi_{-\alpha\mathbf{k}+\mathbf{q}}(x_1)\chi^{\dagger}_{-\alpha\mathbf{k}_1+\mathbf{q}}(x_1)\chi_{\alpha\mathbf{k}_1}(x),$$

with usual boundary conditions imposed by the continuity of the particle current at the barrier walls:

$$\chi_{\alpha\mathbf{k}}(\pm a/2) = \Psi^{r,l}_{\alpha\mathbf{k}}, \quad \partial_x\chi_{\alpha\mathbf{k}}(\pm a/2) = \partial_x\Psi^{r,l}_{\alpha\mathbf{k}}, \tag{6}$$

where $\Psi^{r,l}_{\alpha\mathbf{k}} \equiv \Psi_{\alpha\mathbf{k}}(\pm a/2)$ are the operators of the right and left systems acting at the barrier boundaries. The eigenstates in the left and right systems can at this stage be arbitrary.

To first order in the interaction the solution of Eq. (5) is

$$\chi_{\alpha\mathbf{k}}(x) = \chi^{(0)}_{\alpha\mathbf{k}}(x) - \sum_{\mathbf{k}_1\mathbf{q}} \frac{\mathcal{V}_{\mathbf{k}-\mathbf{k}_1}}{A} \int_{-\frac{a}{2}}^{\frac{a}{2}} dx_1 dx_2 \times \tag{7}$$
$$\times \mathcal{G}^{(0)}(x,x_1)\chi^{(0)}_{-\alpha\mathbf{k}+\mathbf{q}}(x_2)\chi^{(0)\dagger}_{-\alpha\mathbf{k}_1+\mathbf{q}}(x_2)\chi^{(0)}_{\alpha\mathbf{k}_1}(x_1),$$

where the operators of the non-interactive system

$$\chi^{(0)}_{\alpha\mathbf{k}}(x) = \phi^r(x)\Psi^r_{\alpha\mathbf{k}} + \phi^l(x)\Psi^l_{\alpha\mathbf{k}}, \tag{8}$$
$$\phi^{r,l}(x) = \frac{\sinh(a/2 \pm x)/\lambda}{\sinh(a/\lambda)}, \tag{9}$$

are linear combinations of the two fundamental solutions (9) of unperturbed equation (5). $\mathcal{G}^{(0)}$ is the Green function of the unperturbed equation which can be constructed using $\phi^{r,l}(x)$ as follows:

$$\mathcal{G}^{(0)}(x_1,x_2) = -2m\hbar^{-2}\lambda\sinh(a/\lambda) \times \tag{10}$$
$$\times \begin{cases} \phi^l(x_1)\phi^r(x_2) & x_1 \geq x_2, \\ \phi^l(x_2)\phi^r(x_1) & x_2 \geq x_1, \end{cases}$$

Note that our choice of the integration constants ensures that solution (7) matches the operators of the right $\Psi^r_{\alpha\mathbf{k}}$ and left $\Psi^l_{\alpha\mathbf{k}}$ systems at the boundaries $x = a/2$ and $x = -a/2$ (first boundary condition in Eq. (6)).

Solution (7) is expressed in terms of $\Psi^r_{\alpha\mathbf{k}}$ and $\Psi^l_{\alpha\mathbf{k}}$ and contains no more constants to be determined. Inserting it into the boundary conditions for the derivatives (6) and evaluating the integrals over the coordinates, we find

$$\partial_x \Psi^r_{\alpha\mathbf{k}} = \frac{\Psi^r_{\alpha\mathbf{k}} - 2\mathrm{e}^{-a/\lambda}\Psi^l_{\alpha\mathbf{k}}}{\lambda} - \mathrm{e}^{-a/\lambda}\sum_{\mathbf{k}_1\mathbf{q}} \frac{\tau\mathcal{V}_{\mathbf{k}-\mathbf{k}_1}}{A\hbar} \times$$
$$\times \left(\Psi^l_{-\alpha\mathbf{k}+\mathbf{q}}\Psi^{l\dagger}_{-\alpha\mathbf{k}_1+\mathbf{q}} + \Psi^r_{-\alpha\mathbf{k}+\mathbf{q}}\Psi^{r\dagger}_{-\alpha\mathbf{k}_1+\mathbf{q}}\right)\Psi^l_{\alpha\mathbf{k}_1}, \tag{11}$$

$$\partial_x \Psi^l_{\alpha\mathbf{k}} = \frac{-\Psi^l_{\alpha\mathbf{k}} + 2\mathrm{e}^{-a/\lambda}\Psi^r_{\alpha\mathbf{k}}}{\lambda} + \mathrm{e}^{-a/\lambda}\sum_{\mathbf{k}_1\mathbf{q}} \frac{\tau\mathcal{V}_{\mathbf{k}-\mathbf{k}_1}}{A\hbar} \times$$
$$\times \left(\Psi^l_{-\alpha\mathbf{k}+\mathbf{q}}\Psi^{l\dagger}_{-\alpha\mathbf{k}_1+\mathbf{q}} + \Psi^r_{-\alpha\mathbf{k}+\mathbf{q}}\Psi^{r\dagger}_{-\alpha\mathbf{k}_1+\mathbf{q}}\right)\Psi^r_{\alpha\mathbf{k}_1}, \tag{12}$$

$$\tau = ma\lambda/\hbar = a(m/2U)^{1/2}. \tag{13}$$

These equations now serve as effective microscopic boundary conditions for the right and left operators. Because of the tunneling, the right and left operators are mixed in Eqs. (11) and (12). In the limit $\mathrm{e}^{-a/\lambda} \to 0$, the coupling vanishes:

$$\partial_x \Psi^r_{\alpha\mathbf{k}} = \frac{\Psi^r_{\alpha\mathbf{k}}}{\lambda}, \quad \partial_x \Psi^l_{\alpha\mathbf{k}} = -\frac{\Psi^l_{\alpha\mathbf{k}}}{\lambda}, \tag{14}$$

and the boundary conditions (14) describe isolated right and left systems with the particle current vanishing at both $x = a/2$ and $x = -a/2$. Boundary conditions (14) will be used later to introduce the eigenstates in the isolated right and left systems. When evaluating the integrals over the coordinates we have only taken into account terms linear in $\mathrm{e}^{-a/\lambda} \ll 1$ in Eqs. (11) and (12).

Note that the exchange interaction results in the mixing of the left and right operators with opposite spins in the boundary conditions (11) and (12), which takes into account inelastic spin-flip processes during the tunneling. These terms are proportional to the tunneling time τ (13) assumed to be sufficiently short to justify the use of perturbation theory.

III. TUNNELING CURRENT OPERATOR AND TRANSFER HAMILTONIAN FOR INTERACTING ELECTRONS

Here we use the effective boundary conditions (11) and (12) to derive the microscopic tunneling current operator and transfer Hamiltonian for interacting electrons. Compared to the method pioneered by Prange[18], in our approach both current operator and transfer Hamiltonian will be expressed in terms of the field operators taken at the left, $\Psi^l_{\alpha\mathbf{k}}$ and right, $\Psi^r_{\alpha\mathbf{k}}$ boundaries of the barrier. As in the previous section, we will not use any particular eigenstates in the left and right systems.

As the boundary conditions (11) and (12) conserve the current density, the total current operator $\hat{I}$ can be related to the current density operator at any of the boundaries, for example, at the left one: $\hat{I} = \frac{ie\hbar}{2m}\sum_{\alpha\mathbf{k}}(\partial_x\Psi^{l\dagger}_{\alpha\mathbf{k}}\Psi^l_{\alpha\mathbf{k}} - h.c.)$ with the derivative $\partial_x\Psi^{l\dagger}_{\alpha\mathbf{k}}$ given by boundary condition (12). It can be written as the sum of an elastic and an inelastic contributions: $\hat{I} = \hat{I}_{el} + \hat{I}_{in}$, where

$$\hat{I}_{el} = \frac{ie\mathcal{T}}{\hbar}\sum_{\alpha\mathbf{k}}(\Psi^{r\dagger}_{\alpha\mathbf{k}}\Psi^l_{\alpha\mathbf{k}} - h.c.), \quad \mathcal{T} = \frac{\hbar^2\mathrm{e}^{-a/\lambda}}{m\lambda}, \tag{15}$$

$$\hat{I}_{in} = \frac{ie\mathcal{T}}{\hbar}\sum_{\alpha,\mathbf{k}_2\neq\mathbf{k}_1+\mathbf{q}} \frac{\tau\mathcal{V}_{\mathbf{k}_2-\mathbf{k}_1-\mathbf{q}}}{A\hbar} \times \tag{16}$$
$$\times \frac{\lambda}{2}\Big(\Psi^{r\dagger}_{\alpha\mathbf{k}_2-\mathbf{q}}\Psi^r_{-\alpha\mathbf{k}_2}\Psi^{r\dagger}_{-\alpha\mathbf{k}_1+\mathbf{q}}\Psi^l_{\alpha\mathbf{k}_1} +$$
$$+ \Psi^{r\dagger}_{\alpha\mathbf{k}_1-\mathbf{q}}\Psi^l_{-\alpha\mathbf{k}_1}\Psi^{l\dagger}_{-\alpha\mathbf{k}_2+\mathbf{q}}\Psi^l_{\alpha\mathbf{k}_2} - h.c.\Big).$$

The product $\mathcal{T}\Psi^{r\dagger}_{\alpha\mathbf{k}}\Psi^l_{\alpha\mathbf{k}}$ in Eq. (15) represents the energy operator associated with a one-particle elastic "hopping" between the left and the right systems.

Note that for electrons with close enough wave-vectors

$$|\mathbf{k}_2 - \mathbf{k}_1| \ll (r_S^{-2} + q^2)^{1/2}, \tag{17}$$

the matrix elements of the interaction in Eq. (16) are independent of both $\mathbf{k}_2$ and $\mathbf{k}_1$: $\mathcal{V}_{\mathbf{k}_2-\mathbf{k}_1-\mathbf{q}} \approx \mathcal{V}_{\mathbf{q}}$. Therefore, the sum over $\mathbf{k}_2$ picks up the products of the operators describing simultaneous creation of a hole and an electron with opposite spins. The superpositions of such electron-hole pair operators can be related to *collective spin operators of itinerant electrons* penetrating into the barrier. Let us introduce first the operator of the total spin of the electrons penetrating into a thick barrier ($a \gg \lambda$), say, from the right ferromagnet:

$$S^r_z = \frac{1}{2}\sum_{\mathbf{k}}\int_0^{a/2} dx[\chi^{(0)\dagger}_{\uparrow\mathbf{k}}(x)\chi^{(0)}_{\uparrow\mathbf{k}}(x) - \chi^{(0)\dagger}_{\downarrow\mathbf{k}}(x)\chi^{(0)}_{\downarrow\mathbf{k}}(x)] \approx$$
$$\approx \frac{1}{2}\sum_{\mathbf{k}}\frac{\lambda}{2}[\Psi^{r\dagger}_{\uparrow\mathbf{k}}\Psi^r_{\uparrow\mathbf{k}} - \Psi^{r\dagger}_{\downarrow\mathbf{k}}\Psi^r_{\downarrow\mathbf{k}}]. \tag{18}$$

Here $\chi^{(0)}_{\alpha\mathbf{k}}(x)$ (8) exponentially decays over the distances of the order of λ from the right boundary. At the end of this paper (see, Eq. (41)) we calculate S^r_z and show that it is a macroscopic quantity (much greater than unity), so that it can be treated as a classical spin. Then the operators S^{r+} and S^{r-}, raising and lowering the total

spin S_z^r, can be introduced as

$$S_{\mathbf{q}}^{r+} = \frac{1}{(2|S_z|)^{1/2}} \sum_{\mathbf{k}} \int_0^{a/2} dx \chi_{\uparrow\mathbf{k}-\mathbf{q}}^{(0)\dagger}(x) \chi_{\downarrow\mathbf{k}}^{(0)}(x) \approx$$

$$\approx \frac{1}{(2|S_z|)^{1/2}} \sum_{\mathbf{k}} \frac{\lambda}{2} \Psi_{\uparrow\mathbf{k}-\mathbf{q}}^{r\dagger} \Psi_{\downarrow\mathbf{k}}^{r}, \quad (19)$$

$$S_{\mathbf{q}}^{r-} = \frac{1}{(2|S_z|)^{1/2}} \sum_{\mathbf{k}} \int_0^{a/2} dx \chi_{\downarrow\mathbf{k}-\mathbf{q}}^{(0)\dagger}(x) \chi_{\uparrow\mathbf{k}}^{(0)}(x) \approx$$

$$\approx \frac{1}{(2|S_z|)^{1/2}} \sum_{\mathbf{k}} \frac{\lambda}{2} \Psi_{\downarrow\mathbf{k}-\mathbf{q}}^{r\dagger} \Psi_{\uparrow\mathbf{k}}^{r}. \quad (20)$$

They are normalized in the usual way to satisfy the boson commutation relation: $S_{\mathbf{q}}^{r+} S_{-\mathbf{q}}^{r-} - S_{-\mathbf{q}}^{r-} S_{\mathbf{q}}^{r+} = sign(S_z^r)$. Thus, $S_{\mathbf{q}}^{r+}$ and $S_{-\mathbf{q}}^{r-}$ are the magnon annihilation and creation operators, respectively, for positive S_z^r and vice versa for negative S_z^r.

Keeping in equation (16) only the coherent terms with wave-vectors satisfying inequality (17), one can express the inelastic current in terms of the magnon operators (19) and (20) as

$$\hat{I}_{in} = (2|S_z|)^{1/2} \frac{ie\mathcal{T}}{\hbar} \sum_{\mathbf{kq}} \frac{\tau \mathcal{V}_{\mathbf{q}}}{A\hbar} \Big[(S_{\mathbf{q}}^{r+} + S_{\mathbf{q}}^{l+}) \Psi_{\downarrow\mathbf{k}+\mathbf{q}}^{r\dagger} \Psi_{\uparrow\mathbf{k}}^{l} +$$

$$+ (S_{\mathbf{q}}^{r-} + S_{\mathbf{q}}^{l-}) \Psi_{\uparrow\mathbf{k}+\mathbf{q}}^{r\dagger} \Psi_{\downarrow\mathbf{k}}^{l} - h.c. \Big], \quad (21)$$

where for simplicity $|S_z^r| = |S_z^l| \equiv |S_z|$. Since the operators $S_{\mathbf{q}}^{r,l+}$ and $S_{\mathbf{q}}^{r,l-}$ change the electron spin in the layers of the thickness λ near the barrier boundaries, *the magnons in question are surface ones* with wave-vectors parallel to the interface. In what follows we adopt a harmonic time evolution of the magnon operators $e^{\pm i\omega_{\mathbf{q}}^{r,l} t/\hbar}$ with the parabolic dispersion $\omega_{\mathbf{q}}^{r,l} = D^{r,l} q^2$, where $D^{r,l}$ is the spin stiffness.

In principle, one can solve the equations of motion in the electrodes with effective boundary conditions (11) and (12) treating the tunneling coupling in Eqs. (11) and (12) as a perturbation. Using then these solutions, one can average the products of the left and right operators in the equations for the tunneling current (15) and (21). However, instead of this tedious procedure, it is convenient to derive an effective transfer Hamiltonian and use it for the averaging.

As the tunneling current operator $\hat{I}$ is proportional to the rate of change of the particle number operator of one of the systems (e.g the left one), the transfer Hamiltonian H_T can be formally associated with the operator $\hat{I}$ in the standard way:

$$\hat{I} = -e\dot{\hat{N}}_L = \tfrac{ie}{\hbar}[\hat{N}_L, H_T], \quad (22)$$
$$\hat{N}_L = \textstyle\sum_{\alpha\mathbf{k}} \int\limits_{x \le -a/2} \Psi_{\alpha\mathbf{k}}^{\dagger}(x) \Psi_{\alpha\mathbf{k}}(x) dx.$$

One can easily verify that if the transfer Hamiltonian is taken in the form

$$H_T = - \mathcal{T} \sum_{\alpha\mathbf{k}} (\Psi_{\alpha\mathbf{k}}^{r\dagger} \Psi_{\alpha\mathbf{k}}^{l} + h.c.) - \quad (23)$$

$$- (2|S_z|)^{1/2} \mathcal{T} \sum_{\mathbf{kq}} \frac{\tau \mathcal{V}_{\mathbf{q}}}{A\hbar} \Big[(S_{\mathbf{q}}^{r+} + S_{\mathbf{q}}^{l+}) \Psi_{\downarrow\mathbf{k}+\mathbf{q}}^{r\dagger} \Psi_{\uparrow\mathbf{k}}^{l} +$$

$$+ (S_{\mathbf{q}}^{r-} + S_{\mathbf{q}}^{l-}) \Psi_{\uparrow\mathbf{k}+\mathbf{q}}^{r\dagger} \Psi_{\downarrow\mathbf{k}}^{l} + h.c. \Big],$$

the commutator $[\hat{N}_L, H_T]$ results in the current operator $\hat{I} = \hat{I}_{el} + \hat{I}_{in}$ given by Eqs. (15) and (21). A more tedious calculation allows one to derive H_T directly from the effective boundary conditions (11) and (12) independently of the current operator $\hat{I}$ and make sure that H_T and $\hat{I}$ are automatically related by Eq. (22), which is simply the consequence of the current conservation expressed by the boundary conditions (11) and (12).

The first term in Eq. (23) is the coordinate version of the well-known elastic tunneling Hamiltonian of Ref. 10. Expanding the operators $\Psi_{\alpha\mathbf{k}}^{r,l} \equiv \Psi_{\alpha\mathbf{k}}(\pm a/2)$ in the eigenstates of the isolated right and left systems, one can go over to the momentum representation used in Ref. 10. The advantage of the coordinate representation (23) is that the tunneling matrix element $\mathcal{T}$ (15) is a constant, which makes perturbation theory in the coordinate representation simpler.

The second term in Eq. (23) describes inelastic electron tunneling accompanied by the magnon emission (absorption). It is physically equivalent to that used in Ref. 6. *In our model the electron-magnon coupling in the Hamiltonian* H_T (23) *comes from the exchange interaction of the itinerant electrons mediated by the Coulomb potential and is characterized by the matrix element* $\mathcal{V}_{\mathbf{q}}$ (4) *which depends on the magnon wave-vector* $\mathbf{q}$ *and, therefore, on its energy.*

IV. ELASTIC AND INELASTIC CONTRIBUTIONS TO THE TUNNELING CURRENT

To evaluate the statistical average of the tunneling current one can use standard first order perturbation theory with respect to the transfer Hamiltonian (23) in the same way as in Ref. 6. The voltage drop $|e|V$ between the systems is generated by the difference in the Fermi energies in the left E_F and the right $E_F - |e|V$ ferromagnets. We

will first discuss briefly the elastic contribution I_{el}:

$$I_{el} = \frac{2\pi e^2 V \mathcal{T}^2}{\hbar} \begin{cases} \rho_{MM} + \rho_{mm}, & P, \\ \rho_{mM} + \rho_{Mm}, & AP, \end{cases} \tag{24}$$

$$\rho_{MM} = \sum_{\mathbf{k}} \rho_{lM}(E_F, \mathbf{k}) \rho_{rM}(E_F, \mathbf{k}), \tag{25}$$

$$\rho_{mm} = \sum_{\mathbf{k}} \rho_{lm}(E_F, \mathbf{k}) \rho_{rm}(E_F, \mathbf{k}), \tag{26}$$

$$\rho_{mM} = \sum_{\mathbf{k}} \rho_{lm}(E_F, \mathbf{k}) \rho_{rM}(E_F, \mathbf{k}), \tag{27}$$

$$\rho_{Mm} = \sum_{\mathbf{k}} \rho_{lM}(E_F, \mathbf{k}) \rho_{rm}(E_F, \mathbf{k}). \tag{28}$$

Here $\rho_{r,lM}(E_F, \mathbf{k})$ and $\rho_{r,lm}(E_F, \mathbf{k})$ are the majority (M) and minority (m) local electron spectral densities related to the retarded (R) and advanced (A) electron Green functions *at the boundaries of the ferromagnets*:

$$\rho_{r,l}(E_F, \mathbf{k}) = \frac{\mathcal{G}^A_{r,l}(E_F, \mathbf{k}) - \mathcal{G}^R_{r,l}(E_F, \mathbf{k})}{2\pi i}. \tag{29}$$

They can be taken at the Fermi energy for $|eV| \ll E_F$. As in our case the parallel wave-vector $\mathbf{k}$ is conserved upon the tunneling (coherent tunneling), the current (24) is proportional to the trace of the product of two spectral densities. For parallel (P) magnetizations, it is proportional to $\rho_{MM} + \rho_{mm}$ since the tunneling occurs independently between the majority and minority bands whereas in a junction with antiparallel (AP) magnetizations, carriers tunnel from majority to minority bands (and vice versa) and hence $I_{el} \propto \rho_{mM} + \rho_{Mm}$. The degree of spin-polarization $\mathcal{P} = (I^P_{el} - I^{AP}_{el})/I^P_{el}$ of the elastic current is given by

$$\mathcal{P} = \frac{\rho_{MM} + \rho_{mm} - \rho_{mM} - \rho_{Mm}}{\rho_{MM} + \rho_{mm}} < 1. \tag{30}$$

For incoherent tunneling where the parallel momentum is not conserved, $\mathcal{P}$ would be expressed in terms of the local densities of the states $\sum_{\mathbf{k}} \rho_{r,lM}(E_F, \mathbf{k})$ and $\sum_{\mathbf{k}} \rho_{r,lm}(E_F, \mathbf{k})$ rather than the momentum convolutions of the spectral densities (25)–(28). At the end of this paper we give the expressions for the traces (25)–(28) in terms of the band electron parameters of the ferromagnets (see, Eqs. (39) and (40)).

As to the inelastic current I_{in}, let us first discuss the case of the antiparallel alignment of the magnetic moments where one finds

$$I^{AP}_{in} = \frac{2\pi |S_z e| \mathcal{T}^2}{\hbar} \sum_{\mathbf{q}} \left(\frac{\tau \mathcal{V}_{\mathbf{q}}}{A\hbar} \right)^2 \int d\epsilon d\omega \times \tag{31}$$

$$\times \left[(\rho_{MM}\Omega_r(\omega, \mathbf{q}) + \rho_{mm}\Omega_l(\omega, \mathbf{q})) \; \{ n(\epsilon)[1 - n(\epsilon + |e|V - \omega)][1 + N(\omega)] - [1 - n(\epsilon)] n(\epsilon + |e|V - \omega) N(\omega) \} + \right.$$
$$\left. + (\rho_{MM}\Omega_l(\omega, \mathbf{q}) + \rho_{mm}\Omega_r(\omega, \mathbf{q})) \; \{ n(\epsilon)[1 - n(\epsilon + |e|V + \omega)] N(\omega) - [1 - n(\epsilon)] n(\epsilon + |e|V + \omega)[1 + N(\omega)] \} \right].$$

Here we assume that the majority electrons in the left and the right systems are spin-up (↑) and spin-down (↓) ones, respectively (Fig. 3), and the magnon spectral densities are expressed in terms of the advanced and retarded magnon Green functions as

$$\Omega_{r,l}(\omega, \mathbf{q}) = \frac{\mathcal{D}^A_{r,l}(\omega, \mathbf{q}) - \mathcal{D}^R_{r,l}(\omega, \mathbf{q})}{2\pi i} = \delta(\omega - \omega^{r,l}_{\mathbf{q}}). \tag{32}$$

In general, the combinations of the electron $n(\epsilon)$ and magnon $N(\omega)$ occupation numbers in Eq. (31) describe four magnon-emission processes and four counter processes involving an absorption of a magnon, which is only possible at finite temperatures when $N(\omega) \neq 0$. The emission processes are shown schematically in Fig. 3 for $T = 0$.

The processes in Fig. 3a and 3b correspond to the first term in the square brackets in Eq. (31) which determines the current at positive voltages where the Fermi energy in the left system is higher than that in the right one. The process in Fig. 3a has been already discussed in the introduction for the case of half-metallic ferromagnets (Fig. 1). As both initial and final electron states belong to the majority bands, the corresponding contribution to the current is proportional to ρ_{MM} (25) and the magnon spectral density at the right side of the junction Ω_r (32). Note that the similar interaction of the minority electrons cannot give rise to the magnon emission because it would result in the magnetic moment of the right system bigger than that in the ground state. However the minority magnon-assisted transport (proportional to ρ_{mm} (26)) can be realised in a way shown in Fig. 3b: In the course of the exchange scattering, a hot minority (spin-down) electron from the left side excites a majority (spin-up) electron from the same side above the Fermi level of the right system enabling the latter to occupy an empty state in the spin-up (minority) conduction band in the right ferromagnet. At the same time, a spin-wave excitation of the majority (spin-up) Fermi sea is created on the left side of the junction, and the corresponding contribution to the current (31) is proportional to the magnon spectral density at the left boundary Ω_l (32). The processes in Fig. 3c and 3d are generated in

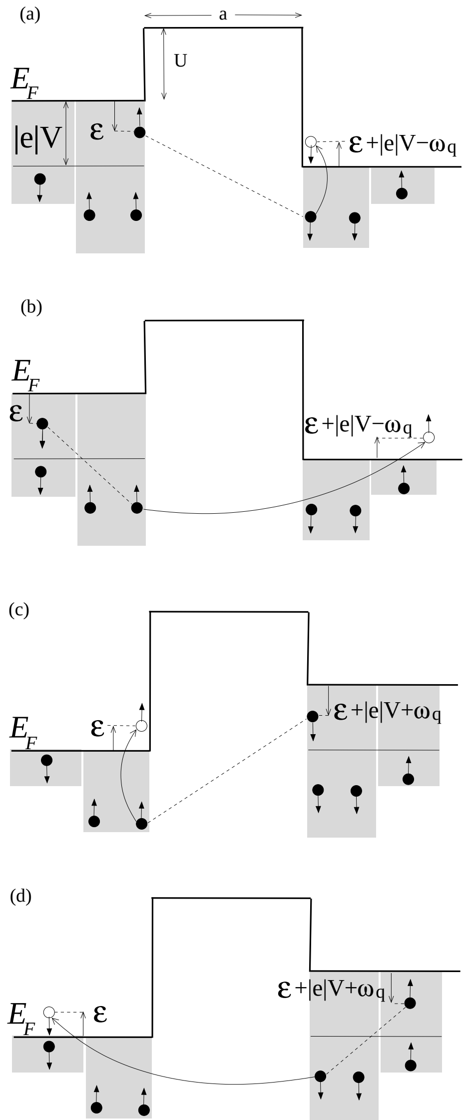

FIG. 3: Exchange-induced spin-flip tunneling between ferromagnets of arbitrary spin-polarization for antiparallel configuration at zero temperature: (a) and (b) – assisted tunneling between the majority and minority bands, respectively, for positive bias voltage $V > 0$, (c) and (d) – same for a negatively biased junction $V < 0$.

negatively biased junctions and described by the second term in the square brackets in Eq. (31). Although they look similar to those shown in Fig. 3a and 3b, in general there is no symmetry because the magnon spectral densities at the left and right boundaries may not be identical: $\Omega_r \neq \Omega_l$.

For the parallel alignment of the magnetic moments, when the majority electrons in both ferromagnets are spin-up ones, one can obtain the following expression for the inelastic current:

$$
\begin{aligned}
I_{in}^{P} = & \frac{2\pi|S_z e|\mathcal{T}^2}{\hbar}\sum_{\mathbf{q}}\left(\frac{\tau\mathcal{V}_{\mathbf{q}}}{A\hbar}\right)^2\int d\epsilon d\omega\, \times \\
& \times(\Omega_r(\omega,\mathbf{q})+\Omega_l(\omega,\mathbf{q}))\,\times \\
& \times\left[\rho_{mM}\ \{n(\epsilon)[1-n(\epsilon+|e|V-\omega)][1+N(\omega)]-\right. \\
& -[1-n(\epsilon)]n(\epsilon+|e|V-\omega)N(\omega)\}\,+ \\
& +\rho_{Mm}\ \{n(\epsilon)[1-n(\epsilon+|e|V+\omega)]N(\omega)- \\
& \left.-[1-n(\epsilon)]n(\epsilon+|e|V+\omega)[1+N(\omega)]\}\right].
\end{aligned}
\tag{33}
$$

Unlike the antiparallel alignment (see, Eq. (31)), in this case the magnon-assisted transport is due to the exchange between a minority electron and a majority one. The latter can be either from the opposite or the same side of the junction, which explains why the current (33) contains the sum $\Omega_r(\omega,\mathbf{q})+\Omega_l(\omega,\mathbf{q})$ of the magnon spectral densities and is proportional to the trace in the momentum space of the product of the minority and the majority electron spectral densities (27) and (28).

In what follows we present the inelastic tunneling spectra for a simpler case of identical ferromagnets. When evaluating the second derivative of the tunneling current, one finds that the equilibrium magnon occupation numbers $N(\omega)$ drop out of the expression for d^2I/dV^2. Only the non-equilibrium processes of magnon-emission contribute to the tunneling spectra:

$$
\begin{aligned}
\frac{d^2I^{AP,P}}{dV^2} = & \left|\frac{d^2I^{AP,P}}{dV^2}\right|_{T,V\to 0}\Omega^{-1}\sum_{\mathbf{q}}\frac{\mathcal{V}^2(\mathbf{q})}{\mathcal{V}^2(0)}\int d\epsilon\,\times \\
& \times n'(\epsilon)\left[n'(\epsilon+|e|V-\omega_{\mathbf{q}})-n'(\epsilon+|e|V+\omega_{\mathbf{q}})\right],
\end{aligned}
\tag{34}
$$

where the second derivative in the limit of the zero temperature and voltage determines the amplitude of the response:

$$
\begin{aligned}
\left|\frac{d^2I^{AP}}{dV^2}\right|_{T,V\to 0} = & \frac{2\pi|S_z e^3|\Omega}{\hbar}\,\times \\
& \times\left(\frac{\tau\mathcal{V}(0)}{A\hbar}\right)^2\mathcal{T}^2(\rho_{MM}+\rho_{mm}),
\end{aligned}
\tag{35}
$$

$$
\frac{\left|d^2I^{P}/dV^2\right|_{T,V\to 0}}{\left|d^2I^{AP}/dV^2\right|_{T,V\to 0}} = 1-\mathcal{P},
\tag{36}
$$

with $\Omega = A/4\pi D$ being the density of states of the surface magnons. According to Eqs. (34) and (36), the ratio of the amplitudes of the response is controlled by the degree of spin-polarization of the elastic current (30), which can be used for an independent measurement of the spin-polarization of the tunneling current. At the same time, for identical ferromagnets the shape of the inelastic tunneling spectrum does not depend on the relative alignment of their magnetic moments and the degree of spin-polarization (see, e.g. Fig. 2 for half-metallic ferromagnets).

In Fig. 2 both excitation energy $|e|V$ and k_BT are normalized by the energy of a surface magnon with the wavelength equal to the screening radius Dr_S^{-2}. For $T=0$ the second derivative is discontinuous at $V=0$ (curve A) recovering the zero-bias anomaly due to the emission of surface magnons studied theoretically in Ref. 6. As $|e|V$ increases, the wave-length of the excited magnon, $\sim (|eV|/D)^{1/2}$ becomes shorter and, when it reaches r_S, the electron-magnon coupling in Eq. (34) becomes strongly energy-dependent leading to a $1/|e|V$ decrease in the tunneling spectrum. Finite temperatures (curves B-E) result in the smearing of the zero-bias anomaly due to the counter spin-flip processes (Fig. 1b) which lead to a finite-rate increase in the response at small $|e|V$ and hence to the formation of *two antisymmetric peaks*. In agreement with the experimental data of Refs. 3,8,12,13,14, at relatively low temperatures ($k_BT < Dr_S^{-2}$, curves B and C) the peaks are sharp. As the temperature increases, they broaden and shift towards higher excitation energies (curves D and E). At large $|e|V$ all the curves merge showing a temperature-independent behaviour, also clearly seen in the experiments[3,8]. For the screening radius $r_S \geq a$ the characteristic magnon energy Dr_S^{-2} is much smaller than that related to the Curie temperature of the ferromagnets k_BT_C.

To compare our results with the experimental data of Refs. 3,8,12,13,14, we can estimate the voltage corresponding to the peak positions at low temperatures as $V_P \sim Dr_S^{-2}/|e|$. For $r_S \sim a \sim 10\mathring{A}$ and the spin stiffness in transition metals $D \approx 300-500\, meV \times \mathring{A}^2$ one obtains $V_P \sim 3-5\, mV$. In Refs. 13, 12 and 8 the peaks were observed at $2\, mV$, $12\, mV$ and $17\, mV$, respectively. At the same time, the Curie temperature of the ferromagnets corresponds to the voltage of order of $100\, mV$. The relation (36) between the spin-polarization of the current and the peak intensities for P and AP configurations is also in good agreement with experimental data[12,13].

It remains to calculate the convolutions of the local electron spectral densities ρ_{MM}, ρ_{mm} and ρ_{Mm} (25)–(28) for the isolated right and left systems which are described by the boundary conditions (14) where λ means the electron penetration length into an infinitely thick barrier ($a \to \infty$) of the finite height U. We will do it for the case of identical ferromagnets where it is enough to calculate the local spectral densities at the boundary of one of the electrodes, say, the right one $x = a/2$. Using the expression for the local electron spectral density in terms of the advanced and retarded Green functions (29), one can write

$$\begin{aligned} \rho_{rM,m}(E_F,\mathbf{k}) &= \textstyle\sum_{k_x} \phi^2_{k_x}\left(\frac{a}{2}\right)\delta(E_F - E_{M,m}(k_x,\mathbf{k})) = \\ &= \lambda^2 \textstyle\sum_{k_x} \left(\partial_x \phi_{k_x}\left(\frac{a}{2}\right)\right)^2 \delta(E_F - E_{M,m}(k_x,\mathbf{k})), \end{aligned} \quad (37)$$

where we introduce the eigenstates $\phi_{k_x}(x)$ in the direction perpendicular to the boundary and take into account that they must satisfy the boundary condition $\phi_{k_x}\left(\frac{a}{2}\right) = \lambda\partial_x\phi_{k_x}\left(\frac{a}{2}\right)$ (14) in order to ensure vanishing of the particle current. For an infinitely high barrier ($\lambda \to 0$), this boundary condition becomes a "hard wall" one and hence $\phi_{k_x}(x) = (2/L)^{1/2}\sin k_x(x-a/2)$ with L being the length of the system. For a high enough barrier, we can still use these eigenstates in the second line in equation (37) since the derivative of $\sin k_x(x-a/2)$ at the boundary is finite. $E_{M,m}(k_x,\mathbf{k}) = \frac{\hbar^2(k_x^2+k^2)}{2m} \mp \frac{\Delta}{2}$ is the electron spectrum in the Stoner model with Δ meaning the exchange-induced spin-splitting. Calculating the integral in Eq. (37), one finds

$$\begin{aligned} &\rho_{rM,m}(E_F,\mathbf{k}) = \frac{\lambda^2 m}{\pi\hbar^2}(k^2_{M,m}-k^2)^{1/2}\Theta(k_{M,m}-|k|), \\ &k^2_{M,m} = 2m(E_F \pm \Delta/2), \end{aligned} \quad (38)$$

where $\Theta(x)$ is a step-function. The calculation of the convolutions (25)–(28) of the local electron spectral densities is now straightforward:

$$\rho_{MM,mm} = \frac{2\pi m^2 A}{\hbar^4}(\lambda k_{M,m})^4 \quad (39)$$

$$\begin{aligned} \rho_{Mm} &= \frac{2\pi m^2 A}{\hbar^4}(\lambda k_m)^4 \times \quad (40) \\ &\times \left[\frac{\gamma^{1/2}(\gamma+1)}{2} - \left(\frac{\gamma-1}{2}\right)^2 \operatorname{arccosh}\frac{\gamma+1}{\gamma-1}\right], \\ \gamma &= k_M^2/k_m^2 > 1. \end{aligned}$$

The same trick with the eigenstates can be used to calculate the total spin S_z (18) of the itinerant electrons penetrating into the barrier. It is given at zero temperature by

$$|S_z| = \frac{\lambda^3 A(k_M^5 - k_m^5)}{30(2\pi)^2}. \quad (41)$$

Finally, a strongly nonlinear behaviour of the $I-V$ curves at small bias voltages has been recently observed in ferromagnet/semiconductor/ferromagnet tunnel structures[21]. In order to apply our approach to such systems one needs to take into account both the energy and momentum dependence of the electron penetration length into the barrier λ since the height of the barrier in Ref. 21 is much smaller than the Fermi energy in the ferromagnets unlike the case of oxide junctions[8,12,13,14]. We also did not consider interaction processes in which a hot electron tunnels elastically through the barrier and then emits a magnon in the course of the exchange scattering in the leads[16]. Since the screening of the Coulomb interaction in the leads is much stronger than inside the barrier, the discussed mechanism of the nonmonotonic behaviour of $d^2I(V)/dV^2$ may not work in the bulk of the ferromagnets. Nevertheless, the proposed theory can be extended to account for spin-relaxation in the leads through the bias-energy dependence of the local electron spectral densities (29).

Acknowledgments

The author thanks K. Richter, J. Siewert and D. Weiss for useful discussions. This work was supported by DFG (Forschergruppe 370, teilproject B7).

[1] G.A. Prinz, Physics Today, April, 58 (1995). Science **282**, 1660 (1998), and Refs. therein.
[2] M. Julliere, Phys. Lett. **54A**, 225 (1975).
[3] J.S. Moodera, T.H. Kim, C. Tanaka, and C.H. de Groot, Philos. Mag. **B 80**, 195 (2000).
[4] J.S. Moodera, L.R. Kinder, T.M. Wong, and R. Meservey, Phys. Rev. Lett. **74**, 3273 (1995).
[5] W.J. Gallagher, S.S.P. Parkin, Y. Lu, X. P. Bian, A. Marley, K. P. Roche, R. A. Altman, S. A. Rishton, C. Jahnes, T. M. Shaw, and G. Xiao, J. Appl. Phys. **81**, 3741 (1997), Y. Lu, X. W. Li, G. Xiao, R. A. Altman, W. J. Gallagher, A. Marley, K. Roche, and S. Parkin, J. Appl. Phys. **83**, 6515 (1998).
[6] S. Zhang, P.M. Levy, A.C. Marley, and S.S.P. Parkin, Phys. Rev. Lett. **79**, 3744 (1997).
[7] J.J. Sun, R. C. Sousa, T. T. P. Galvo, V. Soares, T. S. Plaskett, and P. P. Freitas, J. Appl. Phys. **83**, 6694 (1998).
[8] J.S. Moodera, J. Nowak, and R.J.M. van de Veerdonk, Phys.Rev.Lett. **80**, 2941 (1998)
[9] A.M. Bratkovsky, Appl. Phys. Letts. **72**, 2334 (1998).
[10] M. H. Cohen, L. M. Falicov, and J. C. Phillips, Phys. Rev. Lett. **8**, 316-318 (1962).
[11] C. B. Duke,*Tunneling in Solids, Solid State Physics Suppl.* (Academic, New York, 1969).
[12] Y. Ando, J. Murai, H. Kubota, and T. Miyazaki, J. Appl. Phys. **87**, 5209 (2000).
[13] Y. Ando, M. Hayashi, M. Oogane, H. Kubota, and T. Miyazaki, J. Appl. Phys. **93**, 7023 (2003).
[14] J.H. Yu, H.M. Lee, Y. Ando, and T. Miyazaki, Appl. Phys. Lett. **82**, 4735 (2003).
[15] A.H. MacDonald, T. Jungwirth, and M. Kasner, Phys. Rev. Lett. **81**, 705 (1998).
[16] J. Hong and D.L. Mills, Phys. Rev. B **59**, 13840 (1999).
[17] See, e.g., K. Yosida, *Theory of Magnetism*,(Springer-Verlag Berlin Heidelberg New York, 1996).
[18] R. E. Prange, Phys. Rev. **131**, 1083 (1963).
[19] C. Caroli, R. Combescot, P. Nozieres, and D. Saint-James, J.Phys. C **4**, 916 (1971).
[20] T.E. Feuchtwang, Phys. Rev. B **10**, 4121 (1974).
[21] S. Kreuzer, M. Rahm, J. Biberger, R. Pulwey, J. Raabe, D. Schuh, and D. Weiss, Physica E, **16**, 137 (2003).